Author version: *Microchem. J., vol.106; 2013; 263-269*

Ultrafiltration technique in conjunction with competing ligand exchange method for Ni-humics speciation in aquatic environment

Parthasarathi Chakraborty[1*], Melodie Boissel[1, 2], Alice Reuillon[1, 2], P.V.R. Babu[1], G Parthiban[3]

[1*]National Institute of Oceanography (CSIR), India, 176 Lawsons Bay Colony, Pedawaltair, Visakhapatnam, 530017, Andhra Pradesh, India

Phone-91-891-2539180 (Ext 332); Fax: 91-891-2543595, e-mail: pchak@nio.org

[2]Ecole Nationale Supérieure d'Ingénieurs de Limoges, France

[3]National Institute of Oceanography (CSIR), Dona Paula, Goa

Abstract:

The combination of ultrafiltration technique with competing ligand exchange method provides a better understanding of interactions between Ni and different molecular weight fraction of humic acid (HA) at varying pH. This study suggests that the concentrations of aggregated HA (HA with higher molecular weight) become high at acidic condition (lower pH) and the molecular weight of HA gradually decreases with the increasing pH. The disaggreagation property of HA which involves the release of monomers from the surface of the aggregates produces HAs of different intermediate molecular weight with different Ni complexing capacity. It is observed that Ni prefers to form strong complexes with HAs of lower molecular weight at higher pH but it usually forms weak complexes with HA of higher molecular weight.

Key words: Ultrafiltration; competiting ligand exchange method; Ni speciation; Ni-Humics interactions; multi-method approach; dynamic humic acid molecule

1. Introduction:

The interactions between trace metals and DOC determine bioavailability, toxicity and mobility of trace metals in a system [1–6]. Molecular size distribution of DOC have attracted much attention in recent years since the fate and transport of trace metals are found to be partially controlled by the size/molecular weight of dissolved organics [7-9].

Humic substances (mainly composed by humic and fulvic acid), predominant components of DOC in natural waters, are usually supramolecular association of small organic molecules with functional groups for cation binding [10, 11]. It is reported that humic may form relatively large aggregates (by H-bonding and van der Waal's attraction) and these aggregates are able to disaggregate/reaggregate, depending on the nature and concentration of humics and pH of the medium [12–16]. The stability, lability and mobility of metal-humate complexes in natural environments are dependent on aggregational/disaggregational properties of humic substances. In aquatic environment, knowledge of size distribution of DOC and their metal complexing capacity is thus essential to understand mobility and ultimate fate of metal-DOC complexes in natural system. However, there is no single analytical method which can provide definitive structural or functional information about DOC [17–19]. Among non-destructive analytical methods applied for the characterisation of DOC fractions, high pressure size-exclusion chromatography (HP-SEC) [20–23], fluorescence spectroscopy [24–27], specific ultraviolet absorbance (SUVA) [28–30], dialysis [31–34] and ultrafiltration techniques [35–43] appear to be useful

It is well known that in dialysis technique, the test solution is separated by a dialysis membrane, which will allow only solutes of a certain size to diffuse through. However, this technique is time consuming and limits its application in environmental studies.

In size exclusion chromatography, the solutes are separated in chromatographic columns based on their molecular size. Significant errors could be introduced because of the potential chemical interactions among the column packing, the eluent and the organic components [44, 45].

Ultrafiltration technique is a pressure-modified, convective process. This technique uses semi-permeable membranes to separate species by molecular size, shape and/or charge (Amicon, 1995). Ultrafiltration is a relatively cheap, nondestructive and reagent-free technique. Fractionation is achieved by passing the sample solution through different molecular weight cut-off (MWCO) membranes using either serial or parallel procedure. In addition to that the ultrafiltration technique is ca-

pable of processing large volume samples [44]. Ultrafiltration techniques are being widely used for fractionation study of DOC in aqueous phase [35-43].

The development of analytical technique is required for better understanding of metal-dissolved organic carbon (DOC) interactions in aquatic environment. Ultrafiltration technique was used in this study to separate the distributed metal (in this case nickel) in the different molecular weight fraction of Humic Acid (HA) at different pH. Competing ligand exchange (CLE) method which can provide valuable information of Ni-DOC complexes (concentrations and their dissociation rate constants) was applied to understand the nature of interactions between Ni and different molecular weight fractions of HA in aqueous medium. Ultrafiltration technique coupled with competing ligand exchange method was expected to provide more comprehensive picture and insight into the physical and the chemical characteristics of Ni species.

The aim of this study was to combine ultrafiltration technique with competing ligand exchange method to provide a better understanding of Ni–DOC interactions (of different molecular weight) in aqueous medium at varying pH.

2.Materials and methods

2.1 Reagents and materials:

Chelex 100 chelating resin (Sigma-Aldrich, Fluka Analytical, 100–200 mesh, sodium form) was prepared for the kinetic extraction experiment as described by Price et al, 100 cm^3. ICP Standard (Merck Millipore, Germany) containing Ni (10 $mg.dm^{-3}$ each) was used. 60% ultrapure nitric acid (Merck, Dramstadt, Germany) was used to prepare 10% (v/v) nitric acid to wash the filtration unit.

Ultrapure water of resistivity 18.2MΩ cm^{-1} was obtained direct from a Milli-Q Integral water purification system (Millipore, India) ultrapure water system. Screw-cap Teflon bottles were used as reactors and containers for collecting and storing water samples and reagents. These bottles were precleaned by following the procedure described by Chakrabarti et al. [46]. The Teflon reactor was equilibrated with the test solutions before using it for ultrafiltration and kinetic runs.

2.2 Cascade Ultrafiltration.

The separation of the HA with different molecular weight fraction of HA (dissolved phase) was carried out by using an Amicon Ultrafiltration Stirred Cell 8400 (Beverley, MA, USA). The ultrafiltration membranes (regenerated cellulose, diameter of 76mm, Millipore corporation, Billerica,MA)

with a nominal cut off of 300 kDa, 100 kDa, 50 kDa, 30 kDa, 10 kDa, 5 kDa and 1 kDa were used. The ultrafiltration set up is presented in Figure 1.

At each step of the ultrafiltration, 400 cm^3 of the filtered solution was kept (in an acid cleaned Teflon container) for kinetic speciation study. To determine the possible retention of trace elements by chemical reaction with membranes, blank filter tests were performed.

2.3 Competing ligand exchange method

Appropriate amount of wet Chelex 100 chelating resin (1% w/v wet weight) was added to the filtered sample. The mixture was stirred with a Teflon-coated magnetic stirring bar. Samples (1.0 cm^3) were collected during the course of the kinetic experiments after filtration through a 0.22 μm Millex syringe filter. The decrease in the concentration of total dissolved Ni in the sample solution was determined by measuring Ni concentration in each sample by using ICPMS.

2.4 Determination of total metal concentrations by ICPMS

An ICPMS (Thermo FISCHER ICP-MS, X series 2, Germany) was used for the determination of the total metals concentrations. The radio-frequency power was set at 1400W. Plasma gas, auxiliary gas and carrier gas flows were 13, 0.7 and 0.87 $l.min^{-1}$, respectively. The operating condition of ICP-MS has been reported in our previous study [47, 48].

The sensitivity of the ICP-MS instrument was monitored throughout the measurements by analyzing certified reference material (HISS-1, MESS-3, and PACS-2 from the National Research Council Canada) followed by a reagent blank between every 10 samples. If the sensitivity changed more than 5 % during an experiment, a correction factor was used to correct for the drift.

Total Organic Carbon (TOC) was determined by using Total Organic Carbon Analyzer from Shimadzu Corporation. The model used was TOC-VCPH + ASI-V (incorporating magnetic stirrer).

3. Theory:

3.1 KINETIC THEORY

The kinetic model developed by Olson and Shuman [49] has been adapted [50–56] to study the dissociation of a metal complex, ML, where M is a metal ion and L is a macromolecular, polyfunctional complexant, such as a humic substance, having binding sites of different chemical affinities (the charges on M and L have been omitted for simplicity). In the complexant L, the metal M is bound to

multiple sites in L, all of which dissociate independently and simultaneously at a rate that depends on the nature of the functional group, its position on the macromolecules, and the residual charge. The dissociation is assumed to be first-order. Consider an aqueous mixture of *n* components, in which each component, designated ML_i, exists in equilibrium with its dissociation products:

$$ML_i \underset{k_{-1}}{\overset{k_1}{\rightleftharpoons}} M + L_i \qquad \text{(slow)} \quad (1)$$

where k_1 and k_{-1} are the rate constants for the forward and the reverse reactions, respectively. CLEM uses chemical competition with Chelex 100 chelating resin (solid) as the competing ligand. When Chelex is added in sufficient excess it reacts with M as follows:

$$\text{Chelex} + M \underset{k_{-2}}{\overset{k_2}{\rightleftharpoons}} \text{Chelex - M} \qquad \text{(fast)} \quad (2)$$

The model assumes that

1. Reaction (2) is much faster than reaction (1), and

2. [Chelex] >> [M]

Because [Chelex] >> [M], reaction (2) is pseudo-first-order. Since k_2 is large, as has been determined by inductively coupled plasma - mass spectrometry (ICP-MS), and with Chelex in sufficient excess, the condition k_2 [Chelex] >> k_{-1} [L] holds, and the overall reaction

$$\text{Chelex} + ML_i \rightarrow \text{Chelex - M} + L_i \qquad (3)$$

is shifted to the right. Hence, the rate of formation of the M-Chelex complex is determined by the rate of dissociation of ML in reaction (1), and the rate expression is simply:

$$\frac{dC_{\text{M-Chelex}}}{dt} = -\frac{dC_{ML_i}}{dt} = k_1 C_{ML_i} \qquad (4)$$

The two assumptions made above have been fulfilled: the first assumption, by our previous studies using ICP-MS, and the second assumption, by taking a sufficient excess of Chelex 100 chelating resin over the very low concentration of the trace metal ions present in the water samples.

If each complex, ML_i, undergoes, independently and simultaneously, a first-order or pseudo-first-order dissociation reaction, the sum of the concentrations of all components of the complex ML remaining undissociated at time, t, $C(t)$ can be described as:

$$C(t) = \sum_{i=1}^{n} C_i^{\circ} \exp(-k_i t) \qquad (5)$$

where C_i° is the initial concentration of ML_i, the i^{th} component. The $C(t)$ is measured using ICPMS by measuring the uptake of metal ion by Chelex 100 as a function of time.

3.2 Disjunctive and Adjunctive Pathways

The kinetic speciation model described above is based on the assumption that the overall ligand-exchange reactions are primarily influenced by the dissociation of ML. The slow dissociation of ML to give M and L, followed by a fast reaction with the competing ligand, Chelex 100, (equations 1 and 2) is known as the disjunctive pathway. Dissociation of ML is a fundamental process in natural systems. The first-order rate constant of the disjunctive pathway is simply the rate constant for the slow step (equation 1), dissociation of the metal complex, ML. However, it is conceivable that the reactions may proceed via the adjunctive pathway, which is based on direct attack by the competing ligand followed by loss of the original ligand, L, as shown in equations (6) and (7).

$$ML + Chelex \longrightarrow Chelex - M - L \qquad (6)$$

$$Chelex - M - L \longrightarrow M - Chelex + L \qquad (7)$$

The observed rate constants for the adjunctive pathway are strongly influenced by the nature of the arbitrarily chosen probe ligand (i.e. steric and electrostatic factors and by protonation of the incoming ligand) since either formation or dissociation of the intermediate ternary complex can be rate-limiting. Consequently, little relevant information can be inferred about the processes in natural systems from the adjunctive pathway. Both the disjunctive and the adjunctive pathways generally contribute to the observed, overall rate constant; however, conditions may be chosen to so that one pathway predominates. Although the formation of mixed ligand complexes of the type Chelex-M-L (i.e. the adjunctive pathway) has been considered, recent studies indicate that the disjunctive pathway predominates under the experimental conditions used in this work.

4. Results and discussion

4.1 Dynamic (aggregation and disaggregation) behaviour of humic substances at different pH:

According to the new view, humic substances are collections of diverse, relatively low molecular mass components forming dynamic associations stabilized by hydrophobic interactions and hydrogen bonds. However, the intermolecular interactions between the humic components and the pathways by which the associations emerge are not clearly known.

Variation in the structure (size) of humic substances as a function of pH has been reported by Chakraborty [16] using Cd metal as a probe. It has been reported that the increasing pH, start to disaggregate HA to loose some of their building blocks due to the increasing charge density and thus, reduces the size (thus Molecular weight) of humic substances. This process usually opens up new binding sites in the HA molecules. Although the sizes of the HA are related to their charge via protonation and ionic strength effects. However, their swelling and shrinking is largely limited due to their largely branched structure. Recent studies by atomic force microscopy have supported the observation that HS generally exist as small, semi rigid spherocolloids at environmentally relevant pH and ionic strengths.

This study suggests that the changes in pH of the medium have tremendous effects on the aggregation/disaggregation properties of humic substances. Figure 2 shows the variation in concentrations of HA fractions of different molecular weights at different pHs. The concentration (relative percentage) of HA with molecular weight in between 300-30 kDa was highest (18.7%) at pH 5.5. However, the concentrations gradually decreased (0.02%) with the increasing pH to 7.5. This finding suggest that the increasing pH of the medium increase the charge density within the structure of HA and the process of disaggregation of HA increases and HA of lower molecular weight forms. It is evident from Fig. 2 that the relative percentage of HA with molecular weight in between 30-10 kDa gradually decreased with the increasing pH of the medium. The concentrations of HA with molecular weight in between 10-5 kDa gradually increased with the increasing pH from 5.5 to 6 and remained unchanged till pH 7. However, the concentrations of HA of this fraction suddenly decreased when the pH was changed to 7.5.

The variation in concentration of HA (with molecular weight less than 5 kDa) at different pH shows that the concentration of HA with molecular weight less than 5 kDa were relatively high at all the pH (Fig. 2).

The variation in relative concentrations of HA of different molecular weight fraction suggests that HA of higher molecular weight gradually undergoes disaggregation. Aggregated HA molecules first disaggregate to form HA of medium molecular weight. HA of medium molecular weight further undergoes disaggregation to lower molecular weight and so on. It is evident from Fig. 2 that the relative percentage of HA with higher molecular weight (in between 300-30 kDa) gradually decreased with increasing pH and the concentrations of HA of low molecular weight (less than 5 kDa) gradually increased with the increasing pH of the medium. It is interesting to note that the concentrations of HA with medium molecular weight (in between 30-10 and 10-5 kDa) initially were found to increase and then decrease with the further increase in pH. This study suggests that the HA of medium molecular weight were formed as intermediate with the increasing pH of the aquatic system.

A small but significant increase in the diffusion coefficients of the HA has been reported [57] as a function of increasing pH. The mechanism proposed by Marcelo and Wilkinson [57] involves the release of monomers from the surface of the aggregates of HA. It has been reported that pH markedly affect the disaggregation rate of humics. It has been [57] reported that at pH higher than 4.5, the disaggregation rate increases more than 3 orders of magnitude per pH unit increase.

This is the first reported study to understand the dynamic structural behaviour by using simple ultrafiltration technique. Further studies were performed to understand the interactions between nickel(Ni) with humic substances of different molecular weight fraction at different pH.

4.2 Distribution of total nickel with different molecular weight fractions of HA:

Association of Ni with different molecular weight fraction of dissolved HA in model solutions at three different pHs are presented in Fig 3.

The total dissolved concentrations of Ni in the experimental solutions were found to decrease with the separation of HA of different molecular weights from the solutions. These observations suggest that Ni was associated with HA of different molecular weight fractions.

Figure 3 shows that Ni prefers to associate with the HA of low molecular weight (1-5 kDa) followed by the HA of relatively higher molecular weight (10-30 kDa). Approximate 53% of the total dissolved Ni was associated with the lower molecular weight fraction of the HA. However, 20% of the total dissolved Ni was found to associate with the HA of higher molecular weight (above 100 kDa) at pH 6.

The distribution of Ni at pH 7 was found to differ from the distribution observed at pH 6. Approximate 50% of the total dissolved Ni was found to associate with HA of molecular weight varied from 100-10 kDa. It was found that 22% of the total Ni was bound with HA of molecular weight in between 30-50 kDa.

The major fraction of Ni was found to associate with HA with lower molecular weight (10-5 and 5-1 kDa) at pH 8. An approximate 48 and 29% of the total dissolved Ni were found to associate with HA with molecular weight in between 10-5 and <1 kDa. The determination of total Ni concentrations associated with different molecular weight fraction of HA helps us understand the distribution of Ni within the different molecular weight fraction of HA. This study suggests that the different molecular weight fractions of HA had different affinities and complexing capacities for Ni at different pH. However, it is impossible to understand the nature (dynamic or inert) of Ni complexes with different molecular weight fractions of HA. Thus, further investigation was carried out to provide a better understanding of Ni-HA complexes in the model solutions.

4.3 Kinetic speciation of Ni with different molecular weight fraction of HA:

The kinetic curves obtained from the speciation experiments, given in Figs.4, 5 and 6, show the changes in concentrations of dissolved Ni (concentrations of Ni associated with HA) as a function of time in the solution (containing chelex resin as a competing ligand). Each curve displayed an exponential decrease in Ni concentration in the aquatic solution with respect to time. The curved solid lines represent the results from the non-linear regression analysis, and the corresponding numerical results that describe the fitted data are presented in Table 1. Each kinetically-distinguishable component is expressed as a fraction of the total concentrations of Ni in the solutions (i.e. as a percentage of the total Ni concentrations).

The experimental data obtained from the speciation experiments were fitted to a two component model because it was the simplest model that gave an adequate statistical and visual fit to the data (i.e. good representation of the system) [58]. Although use of more components in the model often statistically fit the data better, the additional components were often of negligible concentration or had a high degree of uncertainty.

It is important to note that the two-component system should not be considered to assume that there are only two discrete sediment binding sites, but that it allows for diversity among sites, where the calculated parameters can be thought of as representing average values over a distribution of similar sites with closely-spaced rate constants [58]. Each curve in Figs 3, 4, and 5 show two distinguishable

features: a quickly dropping section that represents the rapid dissociation rate (k_{d1}) of weak Ni-HA complexes (c_1), and the last part of the curve that lies almost parallel to x-axis, which can be attributed to slow dissociation (k_{d2}) of strong Ni-HA complexes (c_2).

4.4 Kinetic speciation of Ni in different molecular weight fractions of HA at pH 6

The speciation parameters of Ni, in Table 1, show that 67% of the total Ni (7.0×10^{-6} M) was dynamic in the unfiltered solution at pH 6. However, the concentration of dynamic complexes of Ni increased with the removal of HA of molecular weight higher than 300 kDa from the experimental solution. It was found that 1.2×10^{-6} M of total Ni were associated with HA of molecular weight higher than 300 kDa. The increase in dynamic Ni complexes with the removal of HA of molecular weight more than 300kDa indicates that Ni probably formed relatively stronger complexes with HA of molecular weight higher than 300 kDa at pH 6.0. The concentration of dynamic complexes of Ni remained almost unchanged even after the removal of HA of different molecular weights (in between 300-50 kDa). This indicates that there was very little association of Ni with HA of molecular weight in between 300-50 kDa at pH 6. However, a major fraction of Ni was found to associate with HA of molecular weight in between 30-10 kDa. The concentrations of dynamic complexes of Ni with HA of molecular weight in between 30-10 kDa were found to be 65% of the total concentrations of Ni. It is interesting to note that the dissociation rate constants of Ni-HA (30-10 kDa) were slow and probably indicating their higher stability. The higher stability of Ni complexes with HA of molecular weight of 30-10 kDa increases the association of Ni in this fraction of HA at pH 6. The association of Ni with HA of molecular weight in between 5-1 kDa was high and the stability of these complexes was high with slow dissociation rate constant (Table 1). A concentration of of Ni (0.91uM) was present in the solution along with HA of molecular weight less than 1 kDa. The major part of total concentration of Ni in this solution was expected to be bioavailable at pH 6.

A major fraction of Ni was mainly associated with three different molecular weight fractions of HA (< 300 kDa, 30-10 kDa and 5-1 kDa). The Ni complexes with HA of molecular weight in between 300-100 kDa were comparatively less stable than the Ni complexes with HA of molecular weight in between 30-10 and 5-1 kDa at pH 6.

It is well known that the binding capacity of metals by HA increases with the increasing pH of the medium. The concentrations of Ni associated with HA of molecular weight higher than 300 kDa was high at pH 6 followed by at pH 7 and the concentration of Ni associated with HA (molecular weight higher than 300 kDa) was found to be lowest at pH 8. Concentrations of Ni associated with HA (of

molecular weight higher than 300 kDa) depend mainly on two factors a) complexing capacity of Ni by HA b) concentration of HA of particular molecular weight at that pH.

At lower pH (pH=6), the aggregational property of HA predominates and the concentrations of HA of higher molecular weight become high. Thus, Ni was found to associate more with HA of higher molecular weight (>300 kDa) at pH 6. At higher pH (pH=8), disaggregational property HA predominates and more metal binding sites become available and thus, Ni associated with HA of lower molecular weight predominate at pH 8. The aggregation/ disaggregation properties and metal binding capacity of HA play a crucial role in controlling distribution of Ni in different molecular weight fraction of HA.

4.5 Kinetic speciation of Ni in different molecular weight fractions of HA at pH 7

The kinetic speciation parameters of Ni-HA (of different molecular weight fraction) at pH 7 (Table 1) show that 54.3% of the total Ni (6.9×10^{-6} M) was dynamic (with dissociation rate constant, k_{d1}, 2.1×10^{-3} s^{-1} in the unfiltered solution at pH 7. The combination of ultrafiltration technique followed by competing ligand exchange method suggests that the nature of Ni complexes with HA of molecular weight higher than 300 kDa were mainly dynamic in nature and 0.6×10^{-6} M of total Ni were associated with HA of molecular weight higher than 300 kDa.

A major fraction of Ni was found to associate with HA of molecular weight in between 30-10 kDa. The higher stability and slow dissociation rate constant (6.8×10^{-4} s^{-1}) of Ni complexes with HA of molecular weight of 30-10 kDa increased the association of Ni with this fraction of HA at pH 7. It is interesting to note that Ni preferred to undergo complexation with HA of molecular weight in between 30-10 kDa both at pH 6 and 7. However, the concentration of Ni associated with HA of molecular weight in between 30-10 kDa at pH 8 was low.

The association of Ni with HA of molecular weight < 1 kDa was high at pH 7. The kinetic extraction study suggests that the stability of Ni-HA (molecular weight less than 1 kDa) complexes was high with slow dissociation rate constants (3.4×10^{-4} s^{-1}) was observed. A concentration of Ni (1.8×10^{-6} M) was present in the solution along with HA of molecular weight less than 1 kDa. The major part of the total concentration of Ni in this solution is expected to be less dynamic in nature compared to the Ni-HA complexes at pH 6. A similar observation was obtained. The dissociation rate constant of Ni-HA complexes (HA of molecular weight lower than 1 kDa) was slower at pH 7 (3.4×10^{-4} s^{-1}) than pH 6 (5.0×10^{-3} s^{-1}). Major fractions of Ni were mainly associated with three different molecular weight fractions of HA (50-30 kDa, 30-10 kDa and <1 kDa) at pH 7.

4.6 Kinetic speciation of Ni in different molecular weight fractions of HA at different 8

The kinetic speciation parameters of Ni-HA (of different molecular weight fraction) at pH 8 are presented in Table 1. It was found that 48% of the total Ni (7.0µM) was dynamic (with dissociation rate constant, k_{d1}, 2.7×10^{-3} s^{-1} in the unfiltered solution at pH 8. The combination of ultrafiltration technique followed by competing ligand exchange method suggests that low concentration of Ni (0.4×10^{-6} M) complexes were associated with HA of molecular weight higher than 300 kDa.

A major fraction of Ni (2.7×10^{-6} M) was found to associate with HA of molecular weight in between 5-10 kDa and 2.0×10^{-6} M of Ni was found to associate with HA of molecular weight less than 1 kDa. The higher stability and slow dissociation rate constant of Ni complexes with HA of molecular weight of 5-10 kDa and <1 kDa of HA increased the association of Ni with this fractions of HA at pH 8. It is interesting to note that Ni preferred to undergo complexation with HA of molecular weight in between 30-10 kDa both at pH 6 and 7. However, the concentration of Ni associated with HA of molecular weight in between 5-10 kDa at pH 8 was high. This is because of the aggregation and disaggregation properties of HA and varying metal complexing capacity of HA at varying pH.

The association of Ni with HA of molecular weight < 5-10 kDa was highest at pH 8 follwed by HA of molecular weight < 1 kDa. The kinetic extraction study suggest that the stability of Ni-HA (molecular weight less than 1 kDa) complexes was high with slow dissociation rate constants. A concentration of Ni (2.0 uM) was present in the solution along with HA of molecular weight less than 1 kDa. Major fractions of Ni were mainly associated with two different molecular weight fractions of HA (5-10 kDa, and <1 kDa).

It is necessary to mention that humic substances are dynamic Combinatorial System of small, flexible molecules and rapidly tumbling molecular fragments that are loosely held together by weak, intermolecular forces in a colloidal state. Hence, the experimentally observed rate constants in these systems may also be influenced by a variety of factors, such as the steric availability of ML and unfolding of the humic molecules, in addition to the dissociation of ML. Coordination sites that are sterically 'hidden' inside humic molecule would proceed via (1) dissociation of ML, (2) diffusion of M out of the molecule, and (3) reaction of M + Chelex. However, these factors would also be expected to affect the results from experimentally measured dissociation rate constants.

The combination of ultrafiltration technique with competing ligand exchange method is providing a better understanding of interactions between Ni and different molecular weight fraction of humic acid (HA) at varying pH. This study suggests that the concentrations of aggregated HA (HA with

higher molecular weight) become high at acidic condition (lower pH). However, the molecular weight of HA gradually decreases with the increasing pH. The disaggreagation property of HA which involve the release of monomers from the surface of the aggregates produces HAs of different intermediate molecular weight with different Ni complexing capacity. It is observed that Ni prefers to form strong complexes with HAs of lower molecular weight at higher pH but it usually forms weak complexes with HA of higher molecular weight.

Acknowledgements

Authors are thankful to the Director, NIO (CSIR), Goa and the Scientist in charge, NIO RC, Waltair for their encouragement and support. Unconditional help from Dr J. N. Pattan from NIO, Goa is gratefully acknowledged. This work is a part of the Council of Scientific and Industrial Research (CSIR) supported OLP 1202. This article bears NIO contribution number xxxx.

References

[1] B. Marschner, K. Kalbitz, Controls of bioavailability and biodegradability of dissolved organic matter in soils. Geoderma, 113 (2003) 211–235.

[2] S.G.S. DePalma, W. Ray Arnold, J.C. McGeer, D. George Dixon, D. Scott Smith, Effects of dissolved organic matter and reduced sulphur on copper bioavailability in coastal marine environments. Ecotoxicol Environ Safety, 74 (2011) 230–237.

[3] L.E. Doig, K. Liber, Influence of dissolved organic matter on nickel bioavailability and toxicity to Hyalella azteca in water-only exposures. Aqua Toxicol, 76 (2006) 203–216.

[4] J.-F. Pan, W.-X. Wang, Influences of dissolved and colloidal organic carbon on the uptake of Ag, Cd, and Cr by the marine mussel Perna viridis. Environ Poll, 129 (2004) 467–477.

[5] J.P. Meador, The interaction of pH, dissolved organic carbon, and total copper in the determination of ionic copper and toxicity. Aqua Toxicol, 19 (1991) 13–31.

[6] J.C. McGeer, C. Szebedinszky, D.G. McDonald, C.M. Wood, The role of dissolved organic carbon in moderating the bioavailability and toxicity of Cu to rainbow trout during chronic waterborne exposure. Comp Biochem Phys C: Toxicol & Pharmacol, 133 (2002) 147–160.

[7] S.A. Wood, The role of humic substances in the transport and fixation of metals of economic interest (Au, Pt, Pd, U, V). Ore Geo Rev, 11 (1996) 1–31.

[8] R.S. Summers, P.K. Cornel, P.V. Roberts, Molecular size distribution and spectroscopic characterization of humic substances. Sci Total Environ, 62 (1987) 27–37.

[9] N.D. Bryan, V.J. Robinson, F.R. Livens, N. Hesketh, M.N. Jones, J.R. Lead, Metal-humic interactions: A random structural modelling approach. Geochim Cosmochim Acta, 61 (1997) 805–820.

[10] F.R. Livens, Chemical reactions of metals with humic material. Environ Poll, 70 (1991) 183–208.

[11] L.A. Warren, E.A. Haack, Biogeochemical controls on metal behaviour in freshwater environments. Earth-Sci Rev, 54 (2001) 261–320.

[12] G. Chilom, A.S. Bruns, J.A. Rice, Aggregation of humic acid in solution: Contributions of different fractions. Organic Geochem, 40 (2009) 455–460.

[13] M. Brigante, G. Zanini, M. Avena, On the dissolution kinetics of humic acid particles. Effect of monocarboxylic acids. Chemosphere, 71 (2008) 2076–2081.

[14] M. Brigante, G. Zanini, M. Avena, Effect of pH, anions and cations on the dissolution kinetics of humic acid particles. Colloids and Surfaces A: Physicochemical and Engineering Aspects, 347 (2009) 180–186.

[15] W. Schimmack, K. Bunzl, Kinetics of disaggregation of humic acid in water. Chemosphere, 8 (1979) 777–785.

[16] P. Chakraborty, Study of cadmium–humic interactions and determination of stability constants of cadmium–humate complexes from their diffusion coefficients obtained by scanned stripping voltammetry and dynamic light scattering techniques. Anal Chim Acta, 659 (2010) 137–143.

[17] A. Matilainen, E.T. Gjessing, T. Lahtinen, L. Hed, A. Bhatnagar, M. Sillanpää, An overview of the methods used in the characterisation of natural organic matter (NOM) in relation to drinking water treatment. Chemosphere, 83 (2011) 1431–1442.

[18] A.P. Deshmukh, C. Pacheco, M.B. Hay, S.C.B. Myneni, Structural environments of carboxyl groups in natural organic molecules from terrestrial systems. Part 2: 2D NMR spectroscopy. Geochim Cosmochim Acta, 71 (2007) 3533–3544.

[19] R. Sihombing, P.F. Greenwood, M.A. Wilson, J.V. Hanna, Composition of size exclusion fractions of swamp water humic and fulvic acids as measured by solid state NMR and pyrolysis-gas chromatography-mass spectrometry. Organic Geochem, 24 (1996) 859–873.

[20] U. Lankes, M.B. Müller, M. Weber, F.H. Frimmel, Reconsidering the quantitative analysis of organic carbon concentrations in size exclusion chromatography. Water Res, 43 (2009) 915–924.

[21] M. Rögner, Chapter 2 Size Exclusion Chromatography, in: Protein Liquid Chromatography. Elsevier, 1999, pp. 89–145.

[22] N. Kawasaki, K. Matsushige, K. Komatsu, A. Kohzu, F.W. Nara, F. Ogishi, M. Yahata, H. Mikami, T. Goto, A. Imai, Fast and precise method for HPLC–size exclusion chromatography with UV and TOC (NDIR) detection: Importance of multiple detectors to evaluate the characteristics of dissolved organic matter. Water Res, 45 (2011) 6240–6248.

[23] M.B. Müller, F.H. Frimmel, A new concept for the fractionation of DOM as a basis for its combined chemical and biological characterization. Water Res, 36 (2002) 2643–2655.

[24] E.H. Goslan, S. Voros, J. Banks, D. Wilson, P. Hillis, A.T. Campbell, S.A. Parsons, A model for predicting dissolved organic carbon distribution in a reservoir water using fluorescence spectroscopy. Water Res, 38 (2004) 783–791.

[25] M. Simonsson, K. Kaiser, R. Danielsson, F. Andreux, J. Ranger, Estimating nitrate, dissolved organic carbon and DOC fractions in forest floor leachates using ultraviolet absorbance spectra and multivariate analysis. Geoderma, 124 (2005) 157–168.

[26] J. Świetlik, E. Sikorska, Application of fluorescence spectroscopy in the studies of natural organic matter fractions reactivity with chlorine dioxide and ozone. Water Res, 38 (2004) 3791–3799.

[27] I. Saadi, M. Borisover, R. Armon, Y. Laor, Monitoring of effluent DOM biodegradation using fluorescence, UV and DOC measurements. Chemosphere, 63 (2006) 530–539.

[28] A.D. Pifer, J.L. Fairey, Improving on SUVA254 using fluorescence-PARAFAC analysis and asymmetric flow-field flow fractionation for assessing disinfection byproduct formation and control. Water Res, 46 (2012) 2927–2936.

[29] M. Hassellöv, Relative molar mass distributions of chromophoric colloidal organic matter in coastal seawater determined by Flow Field-Flow Fractionation with UV absorbance and fluorescence detection. Mar Chem, 94 (2005) 111–123.

[30] T.A. Doane, W.R. Horwáth, Eliminating interference from iron(III) for ultraviolet absorbance measurements of dissolved organic matter. Chemosphere, 78 (2010) 1409–1415.

[31] E.V. Vasyukova, O.S. Pokrovsky, J. Viers, P. Oliva, B. Dupré, F. Martin, F. Candaudap, Trace elements in organic- and iron-rich surficial fluids of the boreal zone: Assessing colloidal forms via dialysis and ultrafiltration. Geochim Cosmochim Acta, 74 (2010) 449–468.

[32] B. Jansen, M.C. Kotte, A.J. van Wijk, J.M. Verstraten, Comparison of diffusive gradients in thin films and equilibrium dialysis for the determination of Al, Fe(III) and Zn complexed with dissolved organic matter. Sci Total Environ, 277 (2001) 45–55.

[33] J.R. Hill, N.J. O'Driscoll, D.R.S. Lean, Size distribution of methylmercury associated with particulate and dissolved organic matter in freshwaters. Sci Total Environ, 408 (2009) 408–414.

[34] M. Baalousha, B. Stolpe, J.R. Lead, Flow field-flow fractionation for the analysis and characterization of natural colloids and manufactured nanoparticles in environmental systems: A critical review. J Chromatogr A, 1218 (2011) 4078–4103.

[35] M.D. Kennedy, H.K. Chun, V.A. Quintanilla Yangali, B.G.J. Heijman, J.C. Schippers, Natural organic matter (NOM) fouling of ultrafiltration membranes: fractionation of NOM in surface water and characterisation by LC-OCD. Desalination, 178 (2005) 73–83.

[36] Y. Ji-xiang, S. Wen-xin, Y. Shui-li, L. Yan, Influence of DOC on fouling of a PVDF ultrafiltration membrane modified by nano-sized alumina. Desalination, 239 (2009) 29–37.

[37] J. Haberkamp, A.S. Ruhl, M. Ernst, M. Jekel, Impact of coagulation and adsorption on DOC fractions of secondary effluent and resulting fouling behaviour in ultrafiltration. Water Res, 41 (2007) 3794–3802.

[38] S. Assemi, G. Newcombe, C. Hepplewhite, R. Beckett, Characterization of natural organic matter fractions separated by ultrafiltration using flow field-flow fractionation. Water Res, 38 (2004) 1467–1476.

[39] A. Chabeaud, L. Vandanjon, P. Bourseau, P. Jaouen, F. Guérard, Fractionation by ultrafiltration of a saithe protein hydrolysate (Pollachius virens): Effect of material and molecular weight cut-off on the membrane performances. J Food Eng, 91 (2009) 408–414.

[40] L. Guo, P.H. Santschi, A critical evaluation of the cross-flow ultrafiltration technique for sampling colloidal organic carbon in seawater. Mar Chem, 55 (1996) 113–127.

[41] P. Burba, B. Aster, T. Nifant'eva, V. Shkinev, B.Y. Spivakov, Membrane filtration studies of aquatic humic substances and their metal species: a concise overview: Part 1. Analytical fractionation by means of sequential-stage ultrafiltration. Talanta, 45 (1998) 977–988.

[42] Y.-D. Xu, D.-B. Yue, Y. Zhu, Y.-F. Nie, Fractionation of dissolved organic matter in mature landfill leachate and its recycling by ultrafiltration and evaporation combined processes. Chemosphere, 64 (2006) 903–911.

[43] E. Bolea, M.P. Gorriz, M. Bouby, F. Laborda, J.R. Castillo, H. Geckeis, Multielement characterization of metal-humic substances complexation by size exclusion chromatography, asymmetrical flow field-flow fractionation, ultrafiltration and inductively coupled plasma-mass spectrometry detection: A comparative approach. J Chrom A, 1129 (2006) 236–246.

[44] B.E. Logan, Q. Jiang, Molecular size distributions of dissolved organic matter. J environ eng 116 (1990) 1046.

[45] G.L. Amy, M.R. Collins, C.J. Kuo, P.H. King, Comparing gel permeation chromatography and ultrafiltration for the molecular weight characterization of aquatic organic matter. J Am Water Works Assoc, 79 (1987) 43–9.

[46] Y. Lu, C.L. Chakrabarti, M.H. Back, D.C. Gregoire, W.H. Schroeder, Kinetic studies of aluminum and zinc speciation in river water and snow. Anal chim acta, 293 (1994) 95–108.

[47] P. Chakraborty, P.V. Raghunadh Babu, V.V. Sarma, A multi-method approach for the study of lanthanum speciation in coastal and estuarine sediments. J Geochem Explor, 110 (2011) 225–231.

[48] P. Chakraborty, P.V.R. Babu, V.V. Sarma, A study of lead and cadmium speciation in some estuarine and coastal sediments. Chem Geol, 294–295 (2012) 217–225.

[49] D.L. Olson, M.S. Shuman, Copper dissociation from estuarine humic materials. Geochim Cosmochim Acta, 49 (1985) 1371–1375.

[50] P. Chakraborty, P.V.R. Babu, V.V. Sarma, A new spectrofluorometric method for the determination of total arsenic in sediments and its application to kinetic speciation. Int J Environ Anal Chem, 92 (2012) 133–147.

[51] P. Chakraborty, *Chemical heterogeneity of humic substances and its impact on metal complexation in natural waters*, Carleton University, 2007.

[52] P. Chakraborty, C.L. Chakrabarti, Chemical speciation of Co, Ni, Cu, and Zn in mine effluents and effects of dilution of the effluent on release of the above metals from their metal–dissolved organic carbon (DOC) complexes. Anal chim acta, 571 (2006) 260–269.

[53] P. Chakraborty, J. Zhao, C.L. Chakrabarti, Copper and nickel speciation in mine effluents by combination of two independent techniques. Anal chim acta, 636 (2009) 70–76.

[55] P. Chakraborty, Y. Gopalapillai, J. Murimboh, I.I. Fasfous, C.L. Chakrabarti, Kinetic speciation of nickel in mining and municipal effluents. Anal. bioanal chem, 386 (2006) 1803–1813.

[56] P. Chakraborty, Speciation of Co, Ni and Cu in the coastal and estuarine sediments: Some fundamental characteristics.J of Geochem Explor, 115 (2012) 13–23.

[57] J. Marcelo, K.J. Wilkinson, Disaggregation kinetics of a peat humic acid: mechanism and pH effects. Environ sci & technol, 36 (2002) 5100–5105.

[58] D.W. Gutzman, C.H. Langford, Kinetic study of the speciation of copper (II) bound to a hydrous ferric oxide. Environ sci & technol, 27 (1993) 1388–1393.

Caption and Legends for figures:

Figure 1. Schematic diagram of the ultrafiltration system.

Figure 2. Dynamic behaviour of humic acid: variation of humic acid concentrations (of different molecular weight) as a function of varying pH.

Figure 3. Concentrations of Ni associated with different molecular weight fraction of humic acid at three different pH.

Figure 4. Nickel-humate complexes (humic acid of different molecular weight) remaining undissociated in the model solutions as function of time, determined by ICP-MS: (○) unfiltered solution; (□), after filtration through 300 kDa; (△), after filtration through 100 kDa; (▽), after filtration through 50 kDa; (◇) after filtration through 30 kDa; (○),after filtration through 10 kDa; (|) after filtration through 5 kDa; (–) after filtration through 1 kDa at T=23±2°C, pH 6.0 ±0.1

Figure 5. Nickel-humate complexes (humic acid of different molecular weight) remaining undissociated in the model solutions as function of time, determined by ICP-MS: (○) unfiltered solution; (□), after filtration through 300 kDa; (△), after filtration through 100 kDa; (▽), after filtration through 50 kDa; (◇) after filtration through 30 kDa; (○),after filtration through 10 kDa; (|) after filtration through 5 kDa; (–) after filtration through 1 kDa. at T=23±2°C, pH 7.0 ±0.1

Figure 6. Nickel-humate complexes (humic acid of different molecular weight) remaining undissociated in the model solutions as function of time, determined by ICP-MS: (○) unfiltered solution; (□), after filtration through 300 kDa; (△), after filtration through 100 kDa; (▽), after filtration through 50 kDa; (◇) after filtration through 30 kDa; (○),after filtration through 10 kDa; (|) after filtration through 5 kDa; (–) after filtration through 1 kDa. at T=23±2°C, pH 8.0 ±0.1

Table 1: Ni speciation at pH 6

Size fraction	Ni_{Total} (M)	c_1 (%)	k_{d1} (s^{-1})	c_2(%)	k_{d2}(s^{-1})
Unfiltered	7.0×10^{-6}	67.1	2.3×10^{-3}	32.9	5.9×10^{-5}
<300KDa	5.8×10^{-6}	84.1	1.2×10^{-3}	15.9	$<1 \times 10^{-6}$
<100KDa	5.2×10^{-6}	89.1	5.1×10^{-3}	10.9	1.4×10^{-4}
<50KDa	5.1×10^{-6}	84.6	8.4×10^{-3}	15.4	1.9×10^{-4}
<30KDa	4.8×10^{-6}	65.1	4.5×10^{-4}	34.9	$<1 \times 10^{-6}$
<10KDa	3.3×10^{-6}	90.8	5.1×10^{-3}	9.2	2.2×10^{-5}
<5KDa	3.1×10^{-6}	67.5	1.6×10^{-4}	32.4	$<1 \times 10^{-6}$
<1KDa	9.1×10^{-7}	78.0	5.0×10^{-3}	22.0	1.5×10^{-5}

Ni speciation at pH 7

Size fraction	Ni_{Total} (M)	c_1	k_{d1}	c_2	k_{d2}
Unfiltered	6.9×10^{-6}	54.3	2.1×10^{-3}	45.7	1.3×10^{-5}
<300KDa	6.3×10^{-6}	50.3	2.6×10^{-3}	49.7	3.2×10^{-5}
<100KDa	5.8×10^{-6}	48.1	1.1×10^{-3}	51.9	1.6×10^{-5}
<50KDa	4.9×10^{-6}	51.2	3.4×10^{-3}	48.8	1.5×10^{-5}
<30KDa	3.4×10^{-6}	59.8	2.5×10^{-3}	41.2	7.5×10^{-5}
<10KDa	2.4×10^{-6}	83.6	6.8×10^{-4}	16.4	$<1 \times 10^{-6}$
<5KDa	2.3×10^{-6}	67.6	6.7×10^{-3}	32.3	1×10^{-5}
<1KDa	1.8×10^{-6}	77.8	3.4×10^{-4}	22.2	$<1 \times 10^{-6}$

Ni speciation at pH 8

Size fraction	Ni_{Total} (M)	c_1	k_{d1}	c_2	k_{d2}
Unfiltered	7.0×10^{-6}	48.0	2.7×10^{-3}	52.9	3.4×10^{-5}
<300KDa	6.6×10^{-6}	65.0	2.9×10^{-2}	34.9	3.2×10^{-5}
<100KDa	6.1×10^{-6}	65.6	9.9×10^{-3}	34.3	3.7×10^{-5}
<50KDa	6.0×10^{-6}	73.1	4.5×10^{-3}	26.1	1.8×10^{-5}
<30KDa	5.9×10^{-6}	72.1	4.7×10^{-3}	27.9	4.2×10^{-5}
<10KDa	5.7×10^{-6}	47.9	9.9×10^{-4}	52.0	$<1 \times 10^{-6}$
<5KDa	2.6×10^{-6}	48.8	2.9×10^{-4}	51.1	$<1 \times 10^{-6}$
<1KDa	2.0×10^{-6}	80.5	7.3×10^{-4}	19.5	$<1 \times 10^{-6}$

All the numbers are the mean of three replicates and the error associated with each numbers were less than 2%

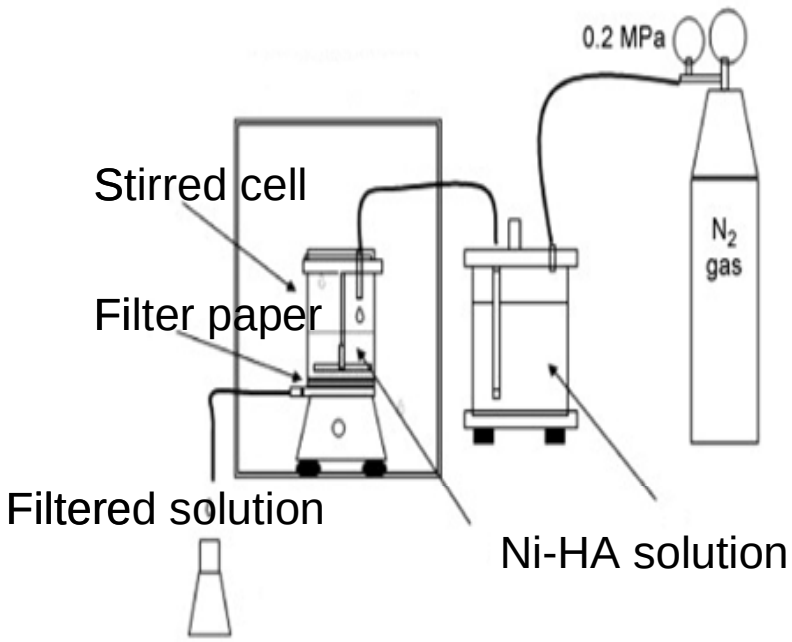
0.2 MPa
Stirred cell
Filter paper
N_2 gas
Filtered solution
Ni-HA solution

Figure 1

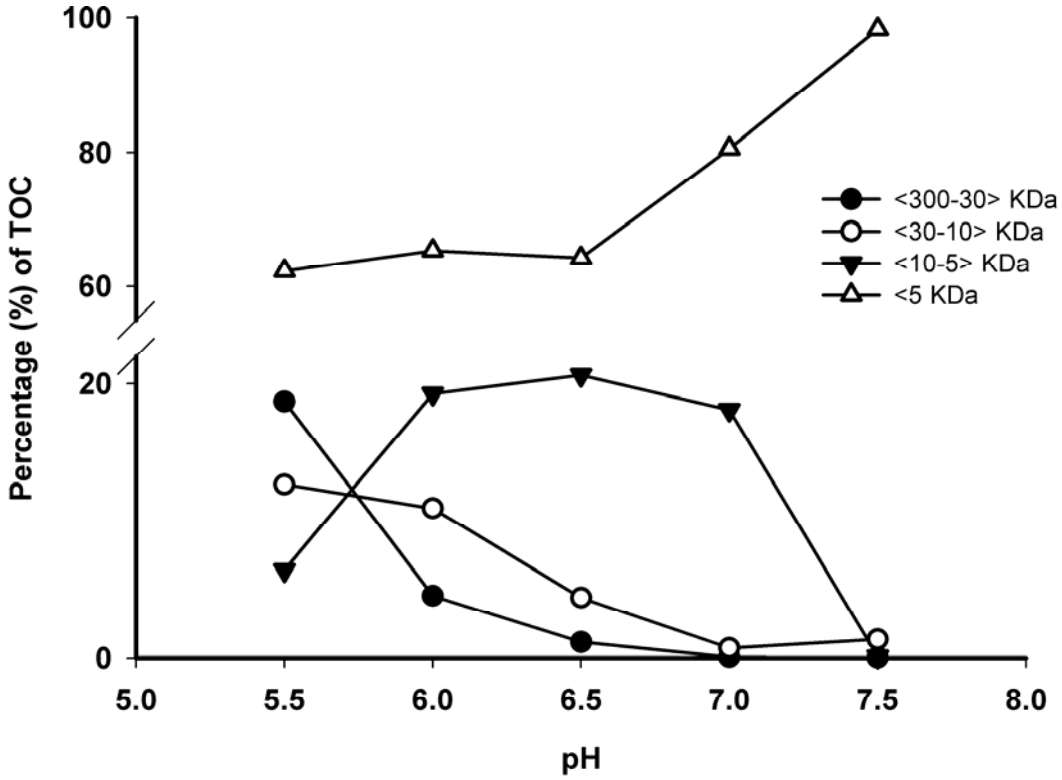
100
80
60
20
0
Percentage (%) of TOC
5.0
5.5
6.0
6.5
7.0
7.5
8.0
pH
<300-30> KDa
<30-10> KDa
<10-5> KDa
<5 KDa

Figure 2

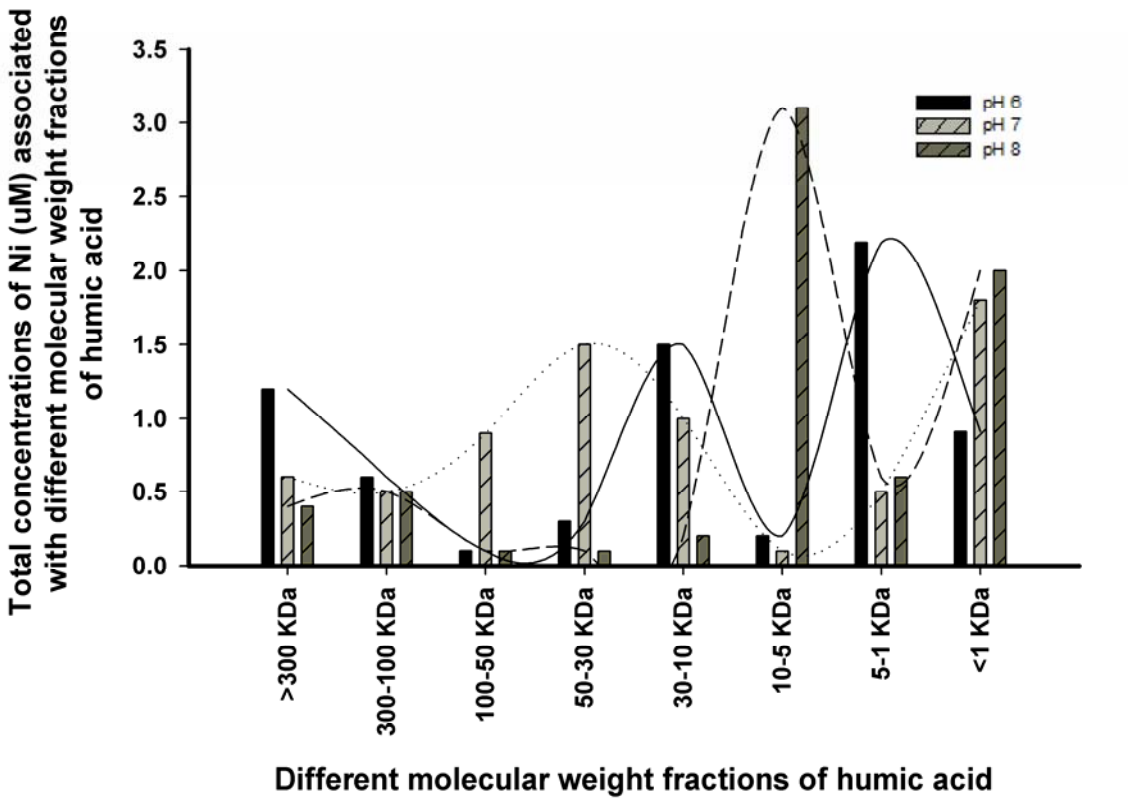
Total concentrations of Ni (uM) associated with different molecular weight fractions of humic acid
3.5
3.0
2.5
2.0
1.5
1.0
0.5
0.0
pH 6
pH 7
pH 8
>300 KDa
300-100 KDa
100-50 KDa
50-30 KDa
30-10 KDa
10-5 KDa
5-1 KDa
<1 KDa
Different molecular weight fractions of humic acid

Figure 3

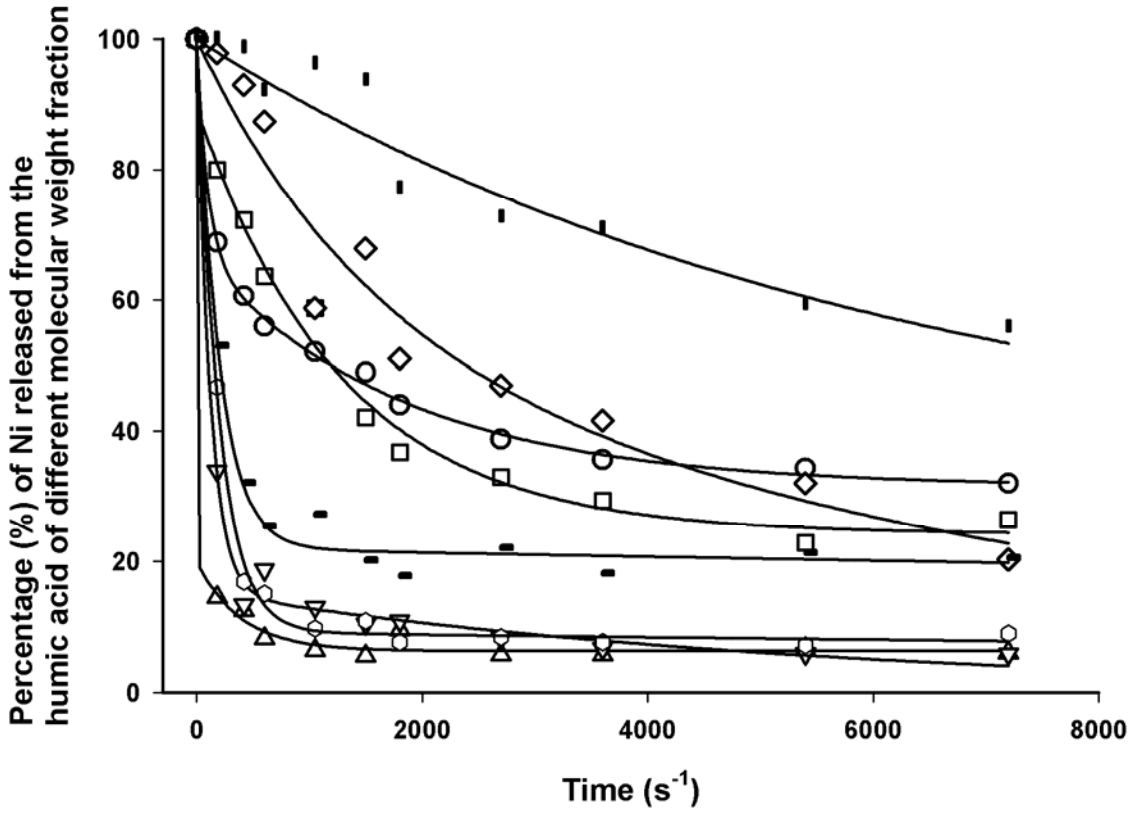
Percentage (%) of Ni released from the humic acid of different molecular weight fraction
100
80
60
40
20
0
0
2000
4000
6000
8000
Time (s-1)

Figure 4

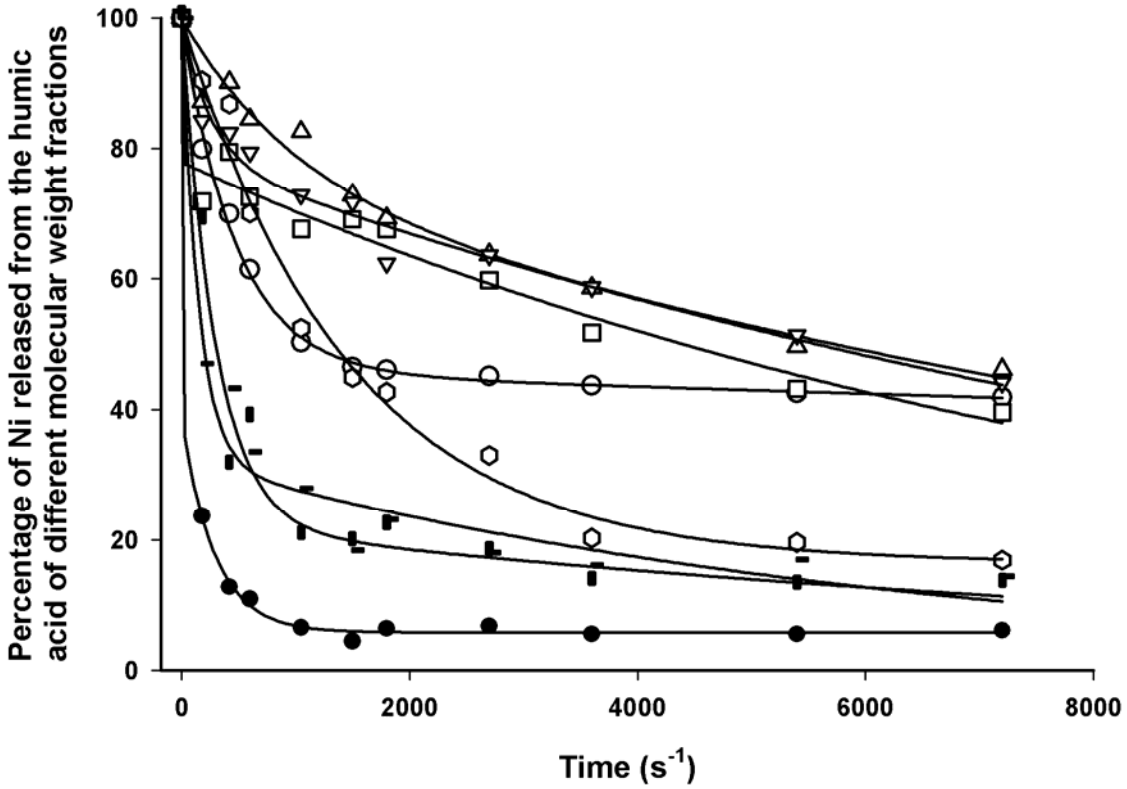
Percentage of Ni released from the humic acid of different molecular weight fractions
100
80
60
40
20
0
0
2000
4000
6000
8000
Time (s-1)

Figure 5

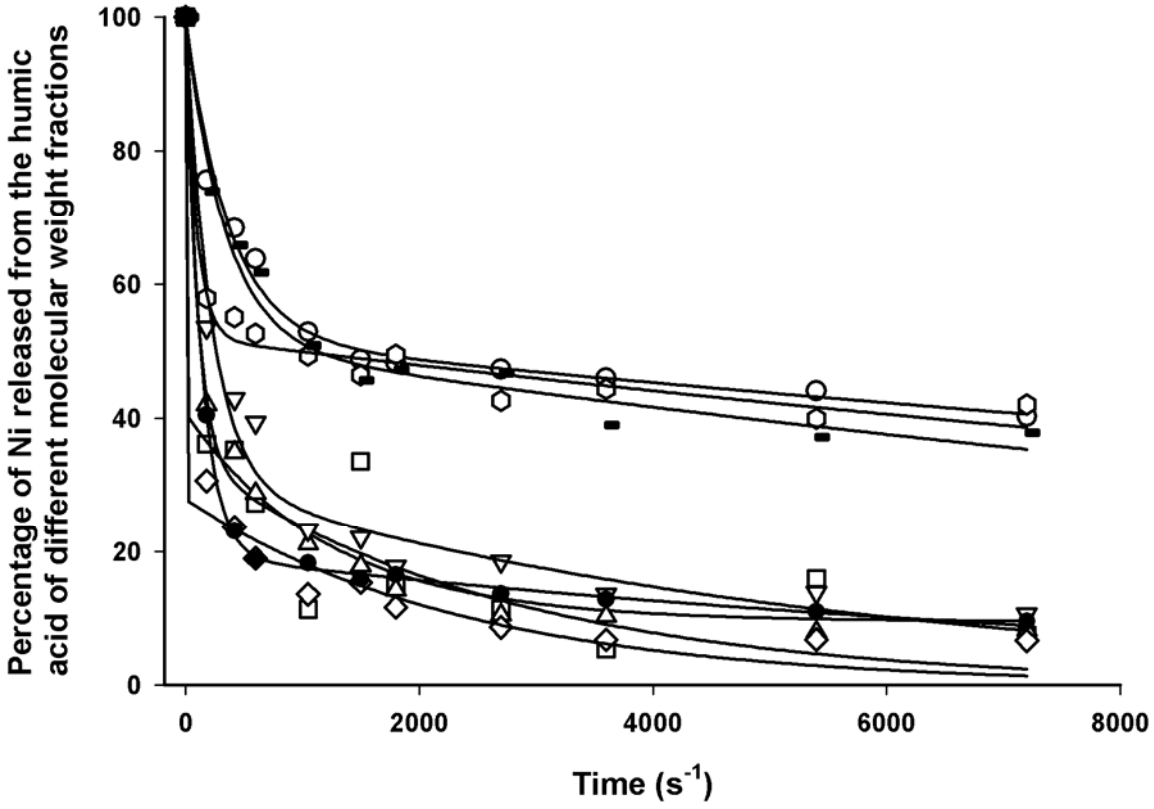
Percentage of Ni released from the humic acid of different molecular weight fractions
100
80
60
40
20
0
0
2000
4000
6000
8000
Time (s-1)

Figure 6